Journal of Alloys and Compounds 525 (2012) 73–77

Contents lists available at SciVerse ScienceDirect

Journal of Alloys and Compounds

journal homepage: www.elsevier.com/locate/jallcom

Improved dehydrogenation properties of lithium alanate ($LiAlH_4$) doped by low energy grinding

Jie Fu[a], Lars Röntzsch[b,*], Thomas Schmidt[b], Thomas Weißgärber[b], Bernd Kieback[a,b]

[a] Dresden University of Technology, Institute for Materials Science, Helmholtzstr. 7, 01069 Dresden, Germany
[b] Fraunhofer Institute for Manufacturing Technology and Advanced Materials (IFAM), Winterbergstr. 28, 01277 Dresden, Germany

ARTICLE INFO

Article history:
Received 2 September 2011
Received in revised form
23 November 2011
Accepted 10 February 2012
Available online xxx

Keywords:
Hydrogen storage material
Lithium aluminum hydride
Grinding
Dehydrogenation
Transition metal catalysts
Thermogravimetry

ABSTRACT

$LiAlH_4$ is an attractive hydrogen storage material because of its high gravimetric hydrogen storage capacity of 10.5 wt.%. There are various reports in the literature on doping $LiAlH_4$ with transition metals in order to improve its dehydrogenation kinetics. However, very often it was found that $LiAlH_4$ starts dehydrogenating already during doping, thereby, reducing the usable hydrogen storage capacity considerably.

In this study, $LiAlH_4$ was doped by low-energy grinding with different transition metal chlorides ($ZrCl_4$, $TiCl_3$ and $NiCl_2$). Thus, unwanted dehydrogenation during doping could be prevented. The positive effect of the dopants on promoting the dehydrogenation of $LiAlH_4$ was systematically studied by thermal analysis. In addition, the crystal phases were characterized by X-ray diffraction. In view of long-term storability of suchlike doped $LiAlH_4$, the weight change was monitored at room temperature up to seven months.

1. Introduction

Hydrogen is an efficient, carbon-free and safe energy carrier. However, its compact and weight-efficient storage is an ongoing subject for research and development [1]. Metal hydrides offer an attractive way for solid-state hydrogen storage with volumetric storage densities up to 150 g-H_2/dm^3 in the case of Mg_2FeH_6 and gravimetric storage densities up to 18 wt.% in the case of $LiBH_4$ [2]. Among metal hydrides, $LiAlH_4$ is particularly attractive because of its high hydrogen capacity (volumetric: 95 g-H_2/dm^3; gravimetric: 10.5 wt.%-H_2) in combination with rather low decomposition temperatures under Ar (onset temperature below 100 °C after doping [3]). Although the reversible reaction from Li_3AlH_6 to $LiAlH_4$ is thought to be endergonic [4], it has been put forward recently that it can be rehydrogenated with the use of polar aprotic solvents under 1 bar hydrogen pressure at room temperature [5], which offers an energy-efficient way for off-board refueling. In any case, $LiAlH_4$ can serve as single-use hydrogen storage material for various special applications, for example, portable hydrogen fuel cell systems.

It is generally accepted that the dehydrogenation of $LiAlH_4$ includes three reaction steps [6]:

$$3LiAlH_4 \rightarrow Li_3AlH_6 + 2Al + 3H_2 \quad (5.3\ \text{wt.\%-}H_2\ \text{of}\ LiAlH_4) \qquad (1.1)$$

$$Li_3AlH_6 \rightarrow 3LiH + Al + (3/2)H_2 \quad (2.6\ \text{wt.\%-}H_2\ \text{of}\ LiAlH_4) \qquad (1.2)$$

$$3LiH + 3Al \rightarrow 3LiAl + (3/2)H_2 \quad (2.6\ \text{wt.\%-}H_2\ \text{of}\ LiAlH_4) \qquad (1.3)$$

Reaction (1.3) is, however, not observed at technically relevant temperature conditions ($T < 250$ °C). Taking step reactions (1.1) and (1.2) into account, $LiAlH_4$ can release up to 7.9 wt.%-H_2 in view of practical applications like hydrogen fuel cells. Although this mechanism has been adopted by most researchers since the early 1970s, a one-step process of the LiH formation without intermediate formation of alkali metal hexahydroaluminate was presented recently by Balema et al. as below [7]:

$$2LiAlH_4 \xrightarrow{Al_3Ti} 2LiH + 2Al + 3H_2 \qquad (1.4)$$

$$2LiH + LiAlH_4 \rightarrow Li_3AlH_6 \qquad (1.5)$$

According to Balema's hypothesis, Li_3AlH_6 is formed in the consecutive reaction (1.5) and collapsed at elevated temperatures (1.2).

Various studies have demonstrated that ball-milling of $LiAlH_4$ together with small quantities of dopants can greatly decrease the temperature for the decomposition of $LiAlH_4$ [3,8–16]. The effect of various dopants on the hydrogen desorption kinetics was reported in the literature. Transition metal (TM) halides, especially titanium chlorides, show the most obvious catalytic effects [9–12,16]. Up to

* Corresponding author. Tel.: +49 351 2537 411; fax: +49 351 2537 399.
E-mail address: Lars.Roentzsch@ifam-dd.fraunhofer.de (L. Röntzsch).

0925-8388/$ – see front matter © 2012 Elsevier B.V. All rights reserved.
doi:10.1016/j.jallcom.2012.02.076

now, the role of TM halides in the decomposition of $LiAlH_4$ is still ambiguous. Since Balema et al. attributed the high catalytic activity of $TiCl_4$ to the in situ formation of a microcrystalline Al_3Ti phase [15], the effect of Al_3Ti and other TM trialuminides on $LiAlH_4$ was investigated [8,17,18].

From the literature reports it can be concluded that doping $LiAlH_4$ by high-energy ball milling causes a serious drawback: $LiAlH_4$ dehydrogenates already during milling of the $LiAlH_4$–dopant mixtures [8–10,14]. Thus, the hydrogen storage capacity available for later use is considerably reduced.

Further, it has to be noted that most studies on the dehydrogenation kinetics of TM-doped $LiAlH_4$ were performed either in vacuum or in argon atmosphere [3,8–12,14,16], which is different from realistic operation conditions where a hydride reservoir should provide hydrogen for a fuel cell at elevated H_2 pressures.

In order to overcome this disadvantage of doping $LiAlH_4$ by ball milling, the purpose of this study was to dope pre-milled $LiAlH_4$ with TMs by low-energy grinding in order to prevent unwanted dehydrogenation during preparation. Three typical TM chlorides ($ZrCl_4$, $TiCl_3$ and $NiCl_2$) were chosen as additives. Their effect on promoting the dehydrogenation properties of $LiAlH_4$ (i.e. reducing the onset temperature of dehydrogenation and enhancing the dehydrogenation rate) and their influence on the total amount of hydrogen released was systematically investigated under a hydrogen back pressure of 1 bar, thereby, simulating realistic operation conditions in combination with hydrogen fuel cells. In this regard, the dehydrogenation of TM-doped $LiAlH_4$ was examined under isothermal conditions at 80 °C, which is the operating temperature of hydrogen fuel cells [19]. Furthermore, the long-term dehydrogenation behavior of TM-doped $LiAlH_4$ at room temperature was monitored up to seven months in order to test its storability.

2. Materials and methods

2.1. General

All samples were prepared and handled in a glovebox (MBraun) under argon (5.0 purity) to prevent unwanted oxidation.

2.2. Materials

Powdery lithium aluminum hydride (99% purity) and zirconium (IV) chloride (98% purity) were purchased from Alfa-Aesar. Titanium (III) chloride (≥98.5% purity) was purchased from Sigma–Aldrich. Nickel (II) chloride hexahydrate (≥98% purity) was obtained from VWR and dehydrated under vacuum for 3 h at 250 °C. The color change from blue to yellow indicated the formation of anhydrous Nickel (II) chloride.

2.3. Pre-milling and doping procedure

As-received $LiAlH_4$ powder was pre-milled for 30 min in a Fritsch P6 using a steel vial and steel balls with a ball-to-powder weight ratio of 20:1 and a rotation speed of 300 rpm. For low-energy doping, the pre-milled $LiAlH_4$ was ground by hand with a pestle in a mortar for 10 min with 2 mol% $ZrCl_4$, $TiCl_3$ and $NiCl_2$, respectively. In addition, 5 mol% $TiCl_3$ was doped into $LiAlH_4$ in the same manner. This 5 mol% $TiCl_3$-doped $LiAlH_4$ was only used for comparison of the dehydrogenation kinetics with the 2 mol% $TiCl_3$-doped $LiAlH_4$ sample (Fig. 5).

2.4. Structural analysis

X-ray diffraction (XRD) was performed with a Bruker D8 Advance using Cu-K_α radiation at a tube voltage of 40 kV and a tube current of 40 mA. The scanning range of the diffraction angle (2θ) was 10–100°. All samples were permanently covered with a capton foil to avoid any unwanted oxidation. The morphology of the powder has been analyzed in an EVO 50 ZEISS scanning electron microscope (SEM) using detectors for back-scattered electrons (BSE).

2.5. Dehydrogenation kinetics

Measurements of dehydrogenation kinetics were carried out in a magnetic suspension balance (Rubotherm) with a precision of 10 μg under a hydrogen (6.0 purity) back pressure of 1 bar. The respective sample mass was about 250 mg. A heating rate of 1 K/min was chosen from 0 °C to 220 °C.

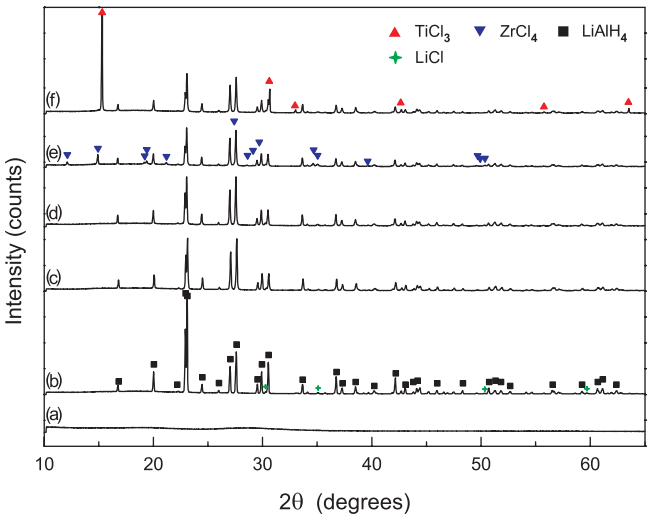

Fig. 1. XRD patterns of (a) dehydrated $NiCl_2$, (b) as-received $LiAlH_4$, (c) pre-milled $LiAlH_4$, (d) $NiCl_2$-doped $LiAlH_4$, (e) $ZrCl_4$-doped $LiAlH_4$ and (f) $TiCl_3$-doped $LiAlH_4$.

2.6. Room temperature dehydrogenation

The freshly doped samples have been kept in gas-tight vials (6 ml) inside an Ar glove box for up to 35 days to test their stability at room temperature (25 °C). The dehydrogenation kinetics was monitored based on the samples' weight loss (sample mass: 1 g) over time via an electronic balance (Sartorius, precision: 1 mg).

3. Results and discussion

3.1. Structure analysis and dehydrogenation properties of TM-doped $LiAlH_4$

Fig. 1 presents the XRD patterns of undoped and freshly TM-doped $LiAlH_4$. LiCl peaks are observed in as-received $LiAlH_4$ as impurity (Fig. 1b). After pre-milling of the $LiAlH_4$ powder for 30 min, no decomposition can be detected (Fig. 1c). The peaks of $ZrCl_4$ and $TiCl_3$ can be easily found in the XRD patterns of $ZrCl_4$-doped $LiAlH_4$ (Fig. 1e) and $TiCl_3$-doped $LiAlH_4$ (Fig. 1f), which indicates that the dopants do not completely react with $LiAlH_4$ under the applied grinding conditions. However, a partial reaction cannot be eliminated owing to the potential formation of nanoparticles and their relatively small molar fraction. The XRD pattern of $NiCl_2$-doped $LiAlH_4$ (Fig. 1d) shows only the characteristic peaks of $LiAlH_4$ but no $NiCl_2$ peaks. This can be explained by the fact that the dehydrated $NiCl_2$ used for doping is amorphous according to the XRD pattern of Fig. 1a. In no case the formation of Li_3AlH_6 was detected which indicates that TM chlorides do not immediately trigger the decomposition of the pre-milled $LiAlH_4$ powder under the low-energy grinding conditions applied here.

SEM investigations reveal that the as-received $LiAlH_4$ powder consists of irregularly shaped particles with a broad size distribution ranging from a few micrometers up to several ten micrometers (Fig. 2a). For comparison, the particle size of pre-milled $LiAlH_4$ doped with different TM chlorides is in the range of several micrometers. For example, Fig. 2(b) exhibits the SEM micrograph of pre-milled $LiAlH_4$ doped with $ZrCl_4$ in BSE mode. Obviously, most of the powder particles are smaller than 10 μm and they are agglomerated. A few large $LiAlH_4$ particles with dimensions in the 30 μm range are still found after pre-milling. The $ZrCl_4$ particles (bright spots in Fig. 2b, exemplarily indicated by arrows) are homogeneously distributed in the $LiAlH_4$ powder bed. Similar results in view of particle size and dopant distribution have been observed for the other samples. Therefore, effects like catalyst distribution

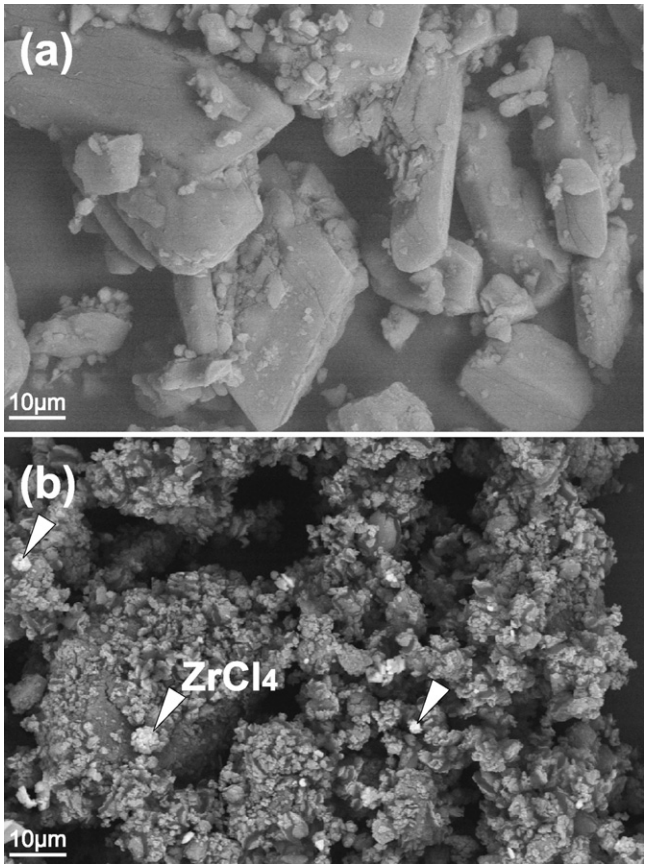

Fig. 2. SEM micrographs in BSE mode of (a) as-received $LiAlH_4$ and (b) pre-milled $LiAlH_4$ doped with $ZrCl_4$. The arrows indicate exemplary $ZrCl_4$ particles.

and particle size are not expected to alter the investigations on the effect of the dopants on $LiAlH_4$.

In Fig. 3 the hydrogen release curves of $LiAlH_4$ doped with different metal chlorides are presented in dependence on time and temperature. The dehydrogenation onset temperature of as-received $LiAlH_4$ is about 140 °C. For pre-milled $LiAlH_4$ and $NiCl_2$-doped $LiAlH_4$, this temperature is reduced by nearly 10 K. It is noteworthy that $ZrCl_4$-doped $LiAlH_4$ already begins to release hydrogen at a temperature of about 80 °C and that $TiCl_3$-doped $LiAlH_4$ starts dehydrogenating at about 65 °C, which refers to an onset temperature drop of 50 K and 65 K, respectively, compared to the pre-milled sample. The maximum amount of hydrogen released

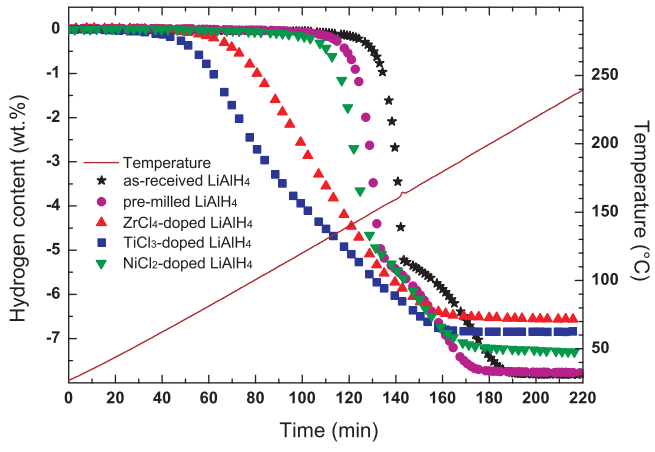

Fig. 3. Dehydrogenation characteristics of $LiAlH_4$ doped with different catalysts.

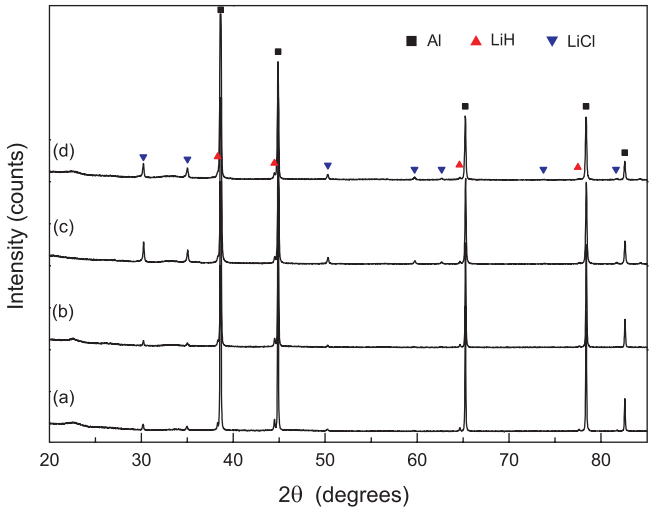

Fig. 4. XRD patterns of (a) dehydrogenated pre-milled and undoped $LiAlH_4$, (b) dehydrogenated $NiCl_2$-doped $LiAlH_4$, (c) dehydrogenated $TiCl_3$-doped $LiAlH_4$ and (d) dehydrogenated $ZrCl_4$-doped $LiAlH_4$.

from $LiAlH_4$ doped with $TiCl_3$, $ZrCl_4$, $NiCl_2$ are 6.81 wt.%, 6.55 wt.% and 7.25 wt.%, respectively. Thus, these materials released 94%, 94% and 99% of their respective theoretical hydrogen capacity considering reactions (1.1) and (1.2). In addition, doping pre-milled $LiAlH_4$ with $TiCl_3$ and $ZrCl_4$ improves the dehydrogenation kinetics significantly. As-received $LiAlH_4$ powder dehydrogenates 90% of its theoretical hydrogen content considering reactions (1.1) and (1.2) within 175 min. In comparison, the pre-milled $LiAlH_4$ and pre-milled $LiAlH_4$ doped with $NiCl_2$, $ZrCl_4$, or $TiCl_3$ release 90% of their theoretical hydrogen content within 163, 157, 154 and 151 min, respectively, during the thermal regime shown in Fig. 3. According to Table 1, the comparison of these results with those from the literature shows that TM-doping of $LiAlH_4$ by low-energy grinding results in improved dehydrogenation properties.

It is worth noting that in the dehydrogenation curves of undoped $LiAlH_4$ and $NiCl_2$-doped $LiAlH_4$ (Fig. 3), two dehydrogenation steps can be easily identified which refer to reactions (1.1) and (1.2). However, in the case of $ZrCl_4$- and $TiCl_3$-doped $LiAlH_4$ the two reaction steps are overlapping which can be explained by Balema' hypothesis of a single-step dehydrogenation [7]. Another possibility is a simultaneous proceeding of reactions (1.1) and (1.2). In situ-synchrotron radiation XRD studies and detailed kinetic investigations are planned to unambiguously identify the reaction sequence in dependence on the dopant.

The disappearance of $LiAlH_4$ and Li_3AlH_6 in the XRD patterns of the dehydrogenated samples (Fig. 4) demonstrates that the decomposition of $LiAlH_4$ to LiH, Al and H_2 has been completed. Interestingly, the TM halides cannot be detected anymore (compare with Fig. 1). Since the intensity of the LiCl peaks has been increased during the dehydrogenations in all TM halide-doped samples, the formation of TM_xAl_y or respective TM can be assumed. However, metallic or intermetallic phases containing any of the TMs, which are considered as the catalytically active compounds [3,7,8,15,17,18] were not detected by XRD in the present study.

For possible practical application for PEM fuel cells, the dehydrogenation properties of $TiCl_3$-doped $LiAlH_4$, which showed the best dehydrogenation performance (Fig. 3), have been examined in further detail up to a maximum temperature of 80 °C (Fig. 5). The results show that $TiCl_3$-doped $LiAlH_4$ can release considerable amounts of hydrogen even at constant 80 °C: 2.9 wt.%-H_2 for 2 mol% and 2.5 wt.%-H_2 for 5 mol% $TiCl_3$-doped $LiAlH_4$. Although the total amount of hydrogen released is a little lower for 5 mol% $TiCl_3$-doped $LiAlH_4$, its dehydrogenation kinetics is clearly faster

Table 1
Dehydrogenation properties of TM chloride-doped $LiAlH_4$ powder.

Dopant	Atmosphere		Dehydrogenation		Heating rate	Maximum temp.	Reference
	Gas	Pressure (Pa)	H_2 released (wt.%)	Onset temp. (°C)	(K/min)	(°C)	
5 wt.% $TiCl_3$	Ar	Not mentioned	~0.3	Not mentioned	2	327	[8]
5 wt.% $ZrCl_4$			~1.1				
5 wt.% VCl_3			~2.7				
5 wt.% $NiCl_2$			~6.4				
5 wt.% $ZnCl_2$			~7.5				
5 mol% $AlCl_3$	Vacuum	0.1	~7.5	~110	8	250	[9]
5 mol% VBr_3			~5.3				
5 mol% VCl_3			~3.0				
2 mol% $TiCl_4$	Ar	10^5	~1.3	>100	3	450	[10]
2 mol% $TiCl_3$			~1.5				
2 mol% $AlCl_3$			~4.6				
2 mol% $FeCl_3$			~2.6				
2 mol% ($TiCl_3 \cdot 1/3\ AlCl_3$)	Ar	Not mentioned	~5.4	~100	2	250	[3]
4 mol% $ZrCl_4$	Not mentioned		~6	~100	7	150	[11]
4 mol% $HfCl_4$			~6				
2 mol% $TiCl_3$	Vacuum	Not mentioned	~2.0	~50	1.3	250	[14]
2 mol% $NiCl_2$	Vacuum	Not mentioned	~6.4	~85	0.3	170	[16]
5 mol% $LaCl_3$	Vacuum	Not mentioned	~5.5	~125	2	250	[12]
5 wt.% $MnCl_2$	H_2	10^5	~7	–	–	170	[20]
2 mol% $TiCl_3$	H_2	10^5	~6.8	~65	1	220	This work
2 mol% $ZrCl_4$			~6.6	~80			
2 mol% $NiCl_2$			~7.3	~130			

during the first 140 min: 1.0 wt.%-H_2 for 2 mol% and 1.5 wt.%-H_2 for 5 mol% $TiCl_3$-doped $LiAlH_4$. The results demonstrate that the concentration of $TiCl_3$ has a significant effect on the decomposition kinetics of $LiAlH_4$, but not on the onset temperature. On the other hand, the increased concentration of $TiCl_3$ reduces the total hydrogen release due to its additional weight and the consumption from the reaction between $LiAlH_4$ and $TiCl_3$.

XRD patterns of $TiCl_3$-doped $LiAlH_4$ after dehydrogenation at 80 °C are shown in Fig. 6. Li_3AlH_6, $TiCl_3$, Al, LiCl and undecomposed $LiAlH_4$ have been found in 2 mol% $TiCl_3$-doped $LiAlH_4$, indicating a partial decomposition of $LiAlH_4$ at 80 °C. Except for the phases found in 2 mol% $TiCl_3$-doped $LiAlH_4$, $TiCl_2$ and an unidentified peak at 14.84° (indicated by red arrow in Fig. 6) are observed in 5 mol% $TiCl_3$-doped $LiAlH_4$. However, unlike the results of [8,15], Al_3Ti has not been observed in both samples and the unidentified peak in 5 mol% $TiCl_3$-doped $LiAlH_4$ is not from Al_3Ti either. It should be noticed that different preparation conditions were applied in [8,15] where Al_3Ti was found (doping by high-energy ball milling with a doping amount of nearly 50 wt.% titanium chloride).

3.2. Long-term dehydrogenation of doped $LiAlH_4$ at room temperature

The freshly doped samples have been kept under Ar atmosphere for up to 35 days to study their long-term stability as a measure for their storability at room temperature. In Fig. 7, the mass changes of the samples are plotted over the 35-day period of investigation. The undoped and pre-milled $LiAlH_4$ did not show any mass change at all during that time. The $NiCl_2$-doped $LiAlH_4$ merely showed a hydrogen release of 0.1 wt.% during 35 days. For $ZrCl_4$- and $TiCl_3$-doped $LiAlH_4$ a respective mass loss of 1.6 and 1.5 wt.% occurred within 35 days. After that, all doped $LiAlH_4$ samples were respectively kept in gas-tight vials for 7 months. During these months all samples kept a constant weight except $ZrCl_4$ doped-$LiAlH_4$ (0.5 wt.% H_2 release).

The dehydrogenation characteristics of the doped-$LiAlH_4$ stored after 7 months are shown in Fig. 8. It should be noticed that here, unlike the dehydrogenation characteristics of $LiAlH_4$ immediately after doping (Fig. 3), the two dehydrogenation steps referring to reactions (1.1) and (1.2) can be easily identified for all the

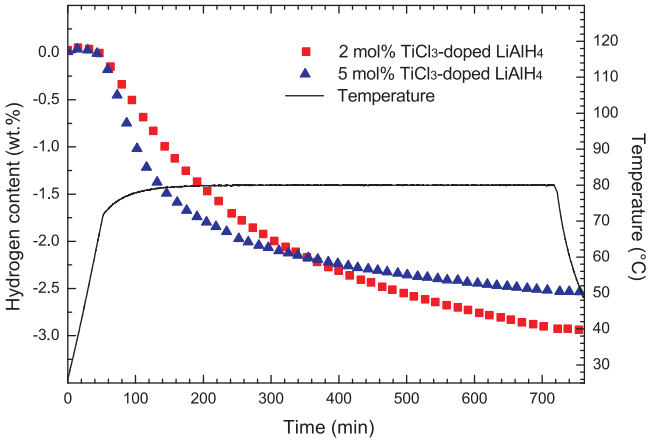

Fig. 5. Dehydrogenation characteristics of $TiCl_3$-doped $LiAlH_4$.

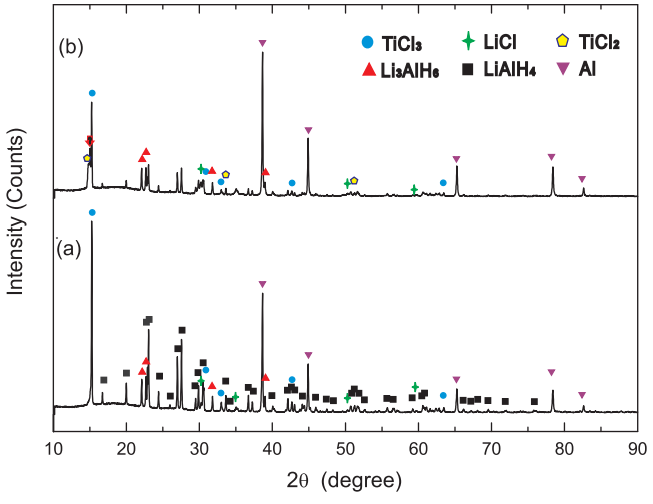

Fig. 6. XRD patterns of (a) 2 mol% $TiCl_3$-doped $LiAlH_4$ after dehydrogenation at 80 °C and (b) 5 mol% $TiCl_3$-doped $LiAlH_4$ after dehydrogenation at 80 °C.

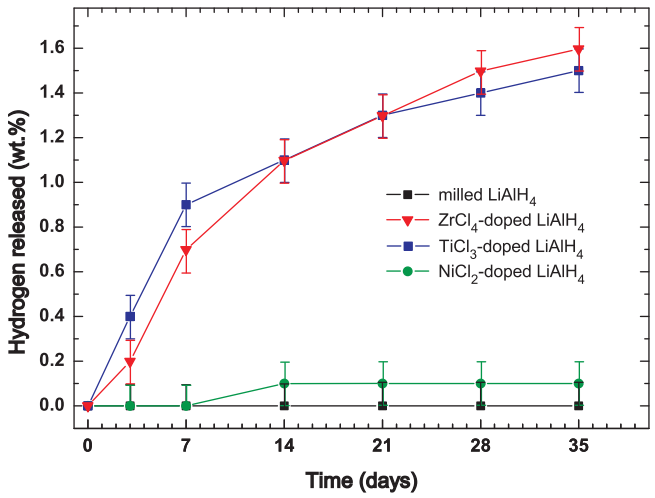

Fig. 7. Dehydrogenation of TM-doped $LiAlH_4$ at room temperature (cf. Section 2.6 for experimental details).

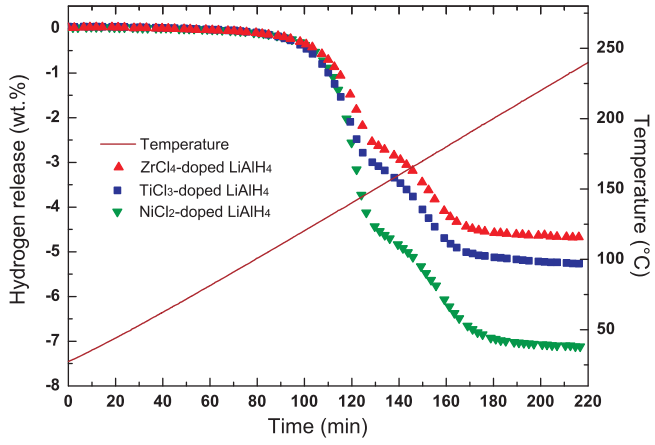

Fig. 8. Dehydrogenation characteristics of doped-$LiAlH_4$ stored at room temperature after seven months.

samples. The respective onset temperatures of both reactions (1.1) and (1.2) are nearly the same for all samples. Comparing Fig. 8 with Fig. 3 one can see that the total amount of hydrogen released differs strongly for $ZrCl_4$- and $TiCl_3$-doped $LiAlH_4$. In other words, doping pre-milled $LiAlH_4$ with $ZrCl_4$ and $TiCl_3$ can trigger the dehydrogenation even at room temperature with a very low reaction rate. Investigations about the influence of the temperature during long term storage on the dehydrogenation properties after the storage period will be reported in a future paper.

4. Conclusions

Doping pre-milled $LiAlH_4$ powder with TM chlorides ($ZrCl_4$, $TiCl_3$ and $NiCl_2$) by low energy grinding can prevent the dehydrogenation of $LiAlH_4$ during the preparation process. Compared to undoped $LiAlH_4$, the dehydrogenation onset temperature of suchlike doped $LiAlH_4$ was dramatically reduced by up to 65 K. In contrast to the findings in the literature more than 90% of the theoretical hydrogen capacity can be released from the TM-doped samples when heating them to 220 °C. At 80 °C almost 3 wt.%-H_2 can be released from $TiCl_3$-doped $LiAlH_4$. $ZrCl_4$ and $TiCl_3$ trigger the decomposition of $LiAlH_4$ powder at room temperature by reaction (1.1). Long-term storage of the $TiCl_3$- and $ZrCl_4$-doped samples leads to a loss of a not insignificant amount of hydrogen. However, about 5 wt.% of hydrogen can still be released from TM-doped $LiAlH_4$ stored for 7 months.

Acknowledgments

Financial support from the Fraunhofer Attract program is gratefully acknowledged. The author Fu Jie thanks the China Scholarship Council for financial support. Furthermore, we thank M. Eckardt, S. Kalinichenka, V. Pacheco and T. Richter for experimental assistance.

References

[1] A. Züttel, Naturwissenschaften 91 (2004) 157–172.
[2] U. Eberle, G. Arnold, R. von Helmolt, J. Power Sources 154 (2006) 456–460.
[3] J. Chen, N. Kuriyama, Q. Xu, H.T. Takeshita, T. Sakai, J. Phys. Chem. B 105 (2001) 11214–11220.
[4] J.W. Jang, J.H. Shim, Y.W. Cho, B.J. Lee, J. Alloys Compd. 420 (2006) 286–290.
[5] J. Graetz, J. Wegrzyn, J.J. Reilly, J. Am. Chem. Soc. 130 (2008) 17790–17794.
[6] J.A. Dilts, E.C. Ashby, Inorg. Chem. 11 (1972) 1230–1236.
[7] V.P. Balema, L. Balema, Phys. Chem. Chem. Phys. 7 (2005) 1310–1314.
[8] Y. Kojima, Y. Kawai, M. Matsumoto, T. Haga, J. Alloys Compd. 462 (2008) 275–278.
[9] J.R. Ares Fernandez, F. Aguey-Zinsou, M. Elsaesser, X.Z. Ma, M. Dornheim, T. Klassen, R. Bormann, Int. J. Hydrogen Energy 32 (2007) 1033–1040.
[10] M. Resan, M. Hampton, J. Lomness, D. Slattery, Int. J. Hydrogen Energy 30 (2005) 1413–1416.
[11] Y. Suttisawat, P. Rangsunvigit, B. Kitiyanan, N. Muangsin, S. Kulprathipanja, Int. J. Hydrogen Energy 32 (2007) 1277–1285.
[12] X.P. Zheng, S.L. Liu, J. Alloys Compd. 481 (2009) 761–763.
[13] V.P. Balema, V.K. Pecharsky, K.W. Dennis, J. Alloys Compd. 313 (2000) 69–74.
[14] D.S. Easton, J.H. Schneibel, S.A. Speakman, J. Alloys Compd. 398 (2005) 245–248.
[15] V.P. Balema, J.W. Wiench, K.W. Dennis, M. Pruski, V.K. Pecharsky, J. Alloys Compd. 329 (2001) 108–114.
[16] T. Sun, C.K. Huang, L.X. Sun, M. Zhu, Int. J. Hydrogen Energy 33 (2008) 6216–6221.
[17] M. Resan, M.D. Hampton, J.K. Lomness, D.K. Slattery, Int. J. Hydrogen Energy 30 (2005) 1417–1421.
[18] J.H. Shim, G.J. Lee, B.J. Lee, Y.J. Oh, Y.W. Cho, Catal. Today 120 (2007) 292–297.
[19] S.J. Peighambardoust, S. Rowshanzamir, M. Amjadi, Int. J. Hydrogen Energy 35 (2010) 9349–9384.
[20] R.A. Varin, L. Zbroniec, J. Alloys Compd. 509 (2012) S736–S739.